Int J Pharm Bio Sci 2012 July; 3(3): (P) 359 - 371

Research Article **Pharmaco Informatics**

International Journal of Pharma and Bio Sciences **ISSN 0975-6299**

SELECTIVITY REQUIREMENT OF ESTROGEN RECEPTOR LIGANDS: MODELING OF FURAN AND PYRAZOLE DERIVATIVES

MD ATAUL ISLAM AND ACHINTYA SAHA*

Department of Chemical Technology, University of Calcutta, 92, A.P.C.Road, Kolkata 700 009, India

ABSTRACT

Chemometric techniques become vital tools in the field of drug discovery by exploring chemical entity with optimistic efficacy. In the present work, a group of non-steroidal ligands, furan and pyrazole derivatives are considered to explore the structural requirement for binding selectivity to estrogen receptor (ER). 2D/3D quantitative structure activity relationship (QSAR) and pharmacophore space modeling studies have been explored for this purpose. The classical QSAR models (R^2_{α}=0.871, Q^2_{α}=0.807, $R^2_{pred\text{-}\alpha}$=0.739; R^2_{β}=0.906, Q^2_{β}=0.876, $R^2_{pred\text{-}\beta}$=0.764) explain that contribution of electronic charges of C_4, C_8 and C_{24} for α-subtype, and C_2, C_{18} and C_{24} of β-subtype are important for binding affinity. In 3D QSAR, field analysis models (CoMFA: R^2_{α}=0.990, Q^2_{α}=0.635, $R^2_{pred\text{-}\alpha}$=0.646; R^2_{β}=0.970, Q^2_{β}=0.544, $R^2_{pred\text{-}\beta}$=0.646) are obtained with importance of steric and electrostatic fields for both subtypes, whereas similarity analysis models (CoMSIA: R^2_{α}=0.995, Q^2_{α}=0.691, $R^2_{pred\text{-}\alpha}$=0.580; R^2_{β}=0.956, Q^2_{β}=0.663, $R^2_{pred\text{-}\beta}$=0.693) revealed that steric, hydrophobic and hydrogen bond (HB) acceptor are prime factors for both α- and β-subtypes. Space modeling studies (R^2_{α}=0.941, Q^2_{α}=0.872, $R^2_{pred\text{-}\alpha}$=0.721; R^2_{β}=0.867, Q^2_{β}=0.831, $R^2_{pred\text{-}\beta}$=0.687) indicate the importance of HB donor and hydrophobic features for both subtypes and aromatic ring for β-subtype for selective binding to the ER. The pharmacophore features obtained from the models are substantiated by molecular docking studies.

KEYWORDS: SERMs, QSAR, CoMFA, CoMSIA, Pharmacophore mapping, Molecular Docking.

ACHINTYA SAHA
Department of Chemical Technology, University of Calcutta, 92, A.P.C.Road, Kolkata 700 009, India, Email: achintya_saha@yahoo.com

INTRODUCTON

The female sex hormone, estrogen secreted by the ovaries and testis with involvement of placenta, adipose tissue, and adrenal glands[1], plays crucial role in development and growth of cell proliferation and differentiation including development of reproductive system and secondary sex characteristics. The hormone replacement therapy (HRT) is most common uses of estrogen agonists in which synthetic estrogens are administered to reduce osteoporotic fractures and improve menopausal symptoms[2], but HRT increases chance of breast and uterus cancers[3,4]. Antagonistic effects of estrogen are used in the treatment of hormone responsive breast cancer and female infertility[5].

The biochemical mechanism of estrogen actions is thought to act primarily by regulating gene expression after binding with estrogen receptor (ER), which belongs to the nuclear receptor super family containing conditional transcription factor[6]. There are two subtypes of ER, namely ER_α and ER_β that exhibit quite similarity in overall structure. ER_α is expressed predominantly in breast and uterine tissues, whereas ER_β is found chiefly in the brain, bone and vascular epithelium[7].

Selective estrogen receptor modulators (SERMs) are structurally diverse synthetic compounds that bind to ER and produce agonistic or antagonistic effects depending upon the target tissue[8,9]. The potent SERMs are being used for numerous estrogen related disorders including hormone-responsive breast cancer[9,10]. Some successful SERMs include tamoxifen, raloxifene and toremifene are classified in generation, suggesting a progressive development in a process intended to improve the beneficial effects while reducing the harmful side effects associated with the earlier SERMs[11].

Rational drug discovery is resource consuming and expensive process. Role of chemometric technique in drug discovery and development is rapidly gaining in popularity, implementation and appreciation[12]. Use of chemometric technique can develop molecules with optimistic efficacy. Considering the immense utility of SERMs for the treatment of post-menopausal diseases, researchers are devoted to develop synthetic therapeutic SERMs for estrogen therapy[13-16]. Chemometric techniques, ligand-based approaches like 2D/3D quantitative structure activity relationship (QSAR) and pharmcophore mapping, and structure-based molecular docking method become vital tools[17] for this purpose. In the present study structure activity relationship (SAR) has been explored using 2D/3D approaches and space modeling studies, i.e. 3D spatial arrangement of ligands for potential binding to active site of receptor. Further, the functionalities developed in SAR and space modeling studies are correlated with structure-based molecular docking study at the catalytic site of the ER.

MATERIALS AND METHODS

Molecular models are derived from a dataset belongs to furan and pyrazole derivatives[18,19] (Figure 1) to explore 2D/3D QSAR and space modeling studies to find out the pharmacophore features of the small molecule required for binding specificity to ER-subtypes. The binding affinity (RBA, Relative binding affinity) for QSAR models is expressed as $kRBA=\log_{10}(100xRBA)$; while $pRBA=(1/RBA)$ is used for space modeling study. The primary objective of the present work is to establish relationship between the structure and corresponding binding affinity through statistical methods, and deduce a pharmacophore map through receptor-independent space modeling technique, and finally derived models are extrapolated with structure-based molecular docking study. The dataset (Table 1) is randomly divided into training set (n=17) containing most and least active compounds for model generation, and test set (n=6) to validate

the derived models. The different statistical parameters considered to assess the models are: R^2 (correlation coefficient), *se* (standard error of estimate), cross-validated variance (CVV) Q^2 (Leave-One-Out (LOO) cross-validated[20] correlation) and *F* (variance ratio) with *df* (degree of freedom). Additionally *EV* (explained variance) for 2D QSAR study, and R^2_{bs} (bootstrapped correlation coefficient) and s_b (standard error of bootstrapped correlation) for 3D QSAR study are considered; while different cost factors are used for space modeling study. To evaluate the predictive power of the model, R^2_{pred} and s_p (standard error of prediction) of the test set are also estimated.

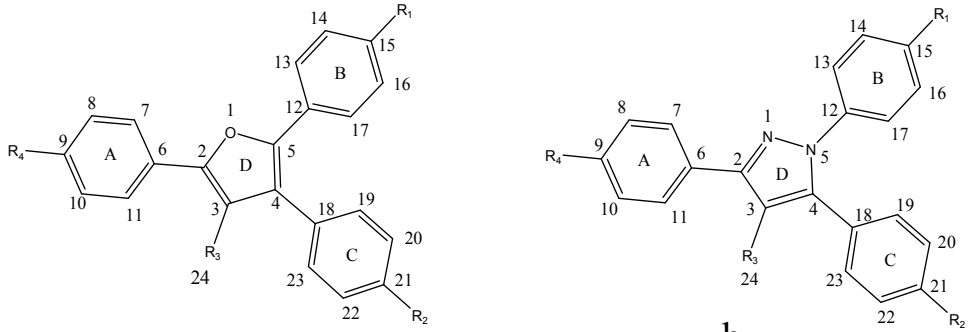

Figure 1
Common structure of (a) furan and (b) pyrazole derivatives. The atoms are numbered through 1 to 24.

Table 1
Structural features and relative binding affinity (RBA) of furan and pyrazole[18,19] analogs

Comp.	R_1	R_2	R_3	R_4	*RBA*	
					ER_α	ER_β
1	OH	OH	CH_3	OH	40.000	0.620
2	OH	OH	C_2H_5	OH	140.000	2.900
3	OH	OH	C_3H_7	OH	100.000	1.800
4	OH	OH	C_4H_9	OH	21.000	3.900
5	OH	OH	*p*-OHC_6H_4	OH	8.700	0.250
6	H	OH	C_2H_5	OH	82.000	7.100
7	H	OH	C_3H_7	OH	140.000	15.000
8	OH	H	C_2H_5	OH	16.500	3.000
9	OH	OH	C_2H_5	H	14.800	4.500
10	H	H	C_2H_5	OH	10.800	3.400
11	H	OH	C_2H_5	H	0.150	0.070
12	OH	H	C_2H_5	H	6.800	2.000
13	H	OH	CH_3	OH	0.760	0.280
14	H	OH	C_2H_5	OH	31.000	1.100
15	H	OH	*n*-C_3H_7	OH	16.800	0.520
16	H	OH	*i*-C_4H_9	OH	56.000	1.400
17	H	OH	*n*-C_4H_9	OH	8.700	0.470
18	OH	OH	C_2H_5	OH	36.000	0.150

19	OH	OH	*n*-C_3H_7	OH	49.000	0.120
20	OH	OH	*i*-C_4H_9	OH	75.000	0.890
21	OH	OH	*n*-C_4H_9	OH	14.000	0.180
22	H	OH	*i*-C_3H_7	OH	5.600	0.860
23	H	OH	C_2H_5	H	0.040	0.060

Molecular scaffold: Comps. 1-12 (Figure 1a), Comps. 13-23 (Figure 1b)

QSAR STUDY

QSAR model is mathematical robust and statistically validated model which attempts to find a statistically significant correlation between chemical structure and biological activity[17]. Different molecular descriptors (electronic, steric, physiochemical and electrotopological) are generated after energy minimization of individual molecule in MOPAC using Austin Model 1 (AM1) for 2D QSAR study. 2D linear models are derived through standard and forward stepwise regression techniques using Statistica[21].

Ligand-based 3D QSAR approaches that include Comparative Molecular Field Analysis (CoMFA)[22] and Comparative Molecular Similarity Indices Analysis (CoMSIA)[23] are reported as effective for understanding of 3D SAR and useful to predict the biological activity before synthesis and animal experiment[24], lead optimization and drug-target interaction. In molecular field analysis (CoMFA), steric ('s) and electrostatic ('e') interaction energies[25] are calculated using Lenard-Jones and Coulombic potentials, and correlated with biological activity of the molecules. In case of CoMSIA study, similarity indices are calculated at regularly placed grid points of pre-aligned molecules using common probe atom. In addition to 's' and 'e', hydrogen bond (HB) acceptor ('a') and donor ('d') along with hydrophobic ('p') fields are calculated[26]. The contour maps of both methods are used to get general insights into the 3D topological features of the binding site.

The molecular alignment is an important step in 3D QSAR to align molecules against each other to maximize the overlap of the pharmacophores to generate molecular fields correctly[27]. If the crystal structure of target proteins is available then molecular docking is the solution of alignment of molecules for development of CoMFA/CoMSIA models. It is reported that docking conformers are appropriately aligning the ligands and developing reliable QSAR models[28,29]. In this purpose, individual molecules of dataset are docked with crystal structure of ERs (PDB ID: 2R6W[30] and 1L2J[31] for α- and β-subtype respectively) obtained from Protein Data Bank[32], and best docked conformer of each compound has been considered for 3D QSAR studies.

In 3D molecular space modeling study, pharmacophore hypothesis can visualize potential interaction between ligand and receptor. To generate the hypothesis, conformational models are developed for each ligand to ensure good coverage of conformational space within a minimal number of conformers using Catalyst[33]. The chemical features considered to explore the spatial pharmacophore maps of this group of compounds are 'a', 'd', 'p', and 'r' (aromatic ring). Different control parameters employed for hypothesis generation are spacing, uncertainty and weight variation[34]. The quality of the hypothesis is adjudged through Fischer's randomization test[33].

DOCKING STUDY

Receptor-based molecular docking study predicts the preferred orientation of ligand and highlights the binding interactions at the active site of the receptor. Docking studies is performed by using LigandFit of receptor-ligand interactions protocol in Discovery Studio[35]. For ligand preparation, all the duplicate structures are removed and ionization change, tautomer generation, isomer generation, Lipinski filter and 3D generator have been set. To prepare receptor, the hydrogen atoms are added to the protein molecules (PDB ID: 2R6W[30] and

1L2J[31] for α- and β-subtypes respectively) and water molecules are removed. The pH of the protein has been set in the range of 6.5 to 8.5. The active site is selected based on the ligand binding domain of the bound ligand. LigandFit is chosen for receptor-ligand interaction and PLP1 is selected as the energy grid. The docking is performed with consideration of electrostatic energy with maximum internal energy 10,000 Cal. No attempt is made to minimize the ligand-receptor complex (rigid docking). After completion of docking, the docked enzyme (protein-ligand complex) is analyzed to investigate the type of interactions. Docked conformers are considered according to their dock score function.

To validate the method, self docking is performed in which bound ligand is docked at the catalytic site of protein molecule and the conformer of the original bound ligand is superimposed to the docked poses to calculate root mean square deviation (RMSD) values. It is reported that low RMSD (<2 Å) value of original bound ligand[36] validate the docking procedure. In the present study, self docking approach is considered for both α- and β-subtypes. The bound ligand conformations in both α- and β-subtypes showed RMSD values 1.553 Å and 0.475 Å respectively.

RESULTS AND DISCUSSION

QSAR Studies

2D QSAR

In the best regressional models, the 95% confidence intervals are shown in parentheses and the *F*-values are significant at the 99% confidence level. The regression constant for the relations is significant at 95%.

The best relationships for ER binding affinity to α-subtype (**Model 1**, R^2=0.871, *se*=0.399, Q^2=0.807, *EV*=84.17, *F(df)*=29.362(3, 13), R^2_{pred}=0.739, s_p=0.239) and β-subtype (**Model 2**, R^2=0.906, *se*=0.241, Q^2=0.876, *EV*=88.45, *F(df)*=41.84(3, 13), R^2_{pred}=0.764, s_p=0.478) are deduced to

$$pRBA_{\alpha} = 8.714(\pm 0.982)HC_4 + 3.897(\pm 1.565)WC_8 - 0.450(\pm 0.182)S_{24} + 1.740(\pm 0.262) \quad \text{Model 1}$$

$$pRBA_{\beta} = 21.337(\pm 5.808)HC_2 + 2.289(\pm 0.326)E_{18} - 2.339(\pm 0.524)WC_{24} + 1.807(\pm 0.370) \quad \text{Model 2}$$

Where, WC_8 and WC_{24} are Wang-Ford charges of C_8 and C_{24} respectively, HC_2 and HC_4 are Huckel charges of C_2 and C_4 respectively, E_{18} is the Electrostatic potential of C_{18}, and S_{24} is the E-state index of C_{24}. The independent variables used in the models (1 and 2) are not intercorrelated (<0.500). The observed vs predicted activity is delineated in Figures 2 and 3 of Models 1 and 2 respectively. More than 93% variance in observed activity with CVV [20] greater than 83% are observed in Models 1 and 2, and indicated the importance of E-state index, Wang-Ford, Huckel charges and electrostatic potential of the molecular scaffold for binding affinity to ER subtypes.

Presence of phenyl rings ('A' and 'C') at C_2 and C_4 positions with R_4 and R_2 substituents (Figure 1) respectively are revealed as crucial for binding affinity in both Models 1 and 2. Negative contribution of E-state index in Model 1 and Wang-Ford charge in Model 2 at C_{24} suggest that presence of electron withdrawing group at this position might be favorable for binding to the receptor for both α- and β-subtypes. Indirect attachment of R_4 substituent increases electron density at C_8 position that enhances binding affinity to α-subtype. It is also observed that presence of electron donating group at C_{18} might be favorable for β-subtype. To verify the predicted ability of selected models, binding affinity of test compounds are predicted. Good correlation between observed and predicted affinity to test compounds in Model 1 (R^2_{pred}=0.739, s_p=0.239) and Model 2 (R^2_{pred}=0.764, s_p=0.478) explain predictive ability and superiority of the models.

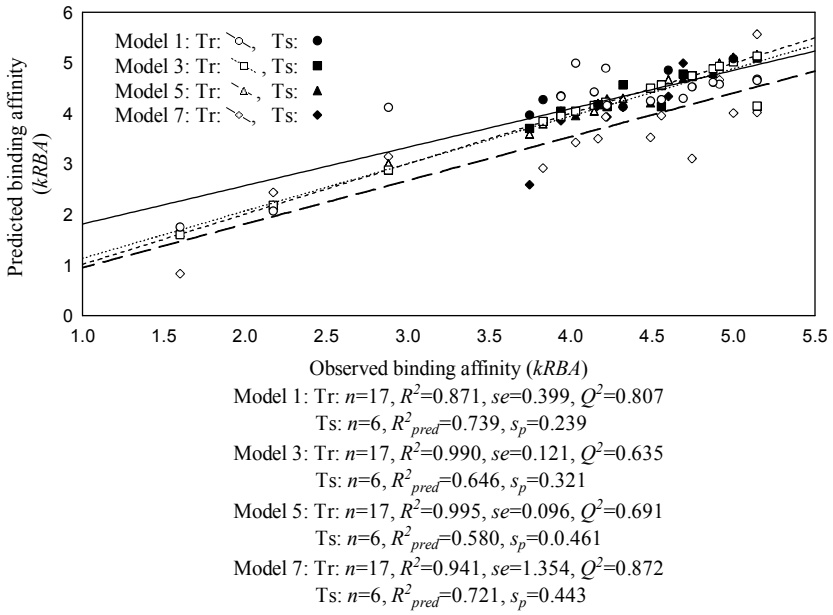

Model 1: Tr: n=17, R^2=0.871, se=0.399, Q^2=0.807
Ts: n=6, R^2_{pred}=0.739, s_p=0.239
Model 3: Tr: n=17, R^2=0.990, se=0.121, Q^2=0.635
Ts: n=6, R^2_{pred}=0.646, s_p=0.321
Model 5: Tr: n=17, R^2=0.995, se=0.096, Q^2=0.691
Ts: n=6, R^2_{pred}=0.580, s_p=0.0.461
Model 7: Tr: n=17, R^2=0.941, se=1.354, Q^2=0.872
Ts: n=6, R^2_{pred}=0.721, s_p=0.443

Figure 2
Observed vs predicted binding affinity as per QSAR and pharmacophore models for ER α-subtype.

3D QSAR STUDY
CoMFA

The best models for α- (**Model 3**, R^2=0.990, se=0.121, Q^2=0.635, R^2_{bs}=0.999, s_b=0.088, R^2_{pred}=0.646, s_p=0.321) and β-subtype (**Model 4**, R^2=0.970, se=0.142, Q^2=0.544, R^2_{bs}=0.982, s_b=0.106, R^2_{pred}=0.646, s_p=0.359) are obtained with high correlation and low error of estimation values. The contributions of features suggest that both 's' (42%) and 'e' (58%) factors in both models are crucial for binding interaction at active site cavity. The predicted activities of Models 3 and 4 are depicted in Figures 2 and 3 respectively. The contour maps of best models suggest that presence of hydroxyl groups at C_{15} in Model 3, and at C_9 and C_{21} in Model 4 along with region around C_4 and C_2 in Models 3 and 4 respectively show positive influence for steric interaction in receptor cavity. But regions around O_1 in Model 3, and C_9, C_{18} and C_{21} positions in Model 4 have negative influence on steric factor for binding affinity. Aromatic rings 'B' and 'C' (Figure 1) in Model 3, hydroxyl groups at C_9 in both models along with region around C_4, C_9, C_{15} and C_{21} accumulate electronic charges which favor electrostatic interactions at catalytic site of the receptor. While region around O_1 for both subtypes, alkyl group at C_3 for α-subtype, and regions around aromatic rings at C_2 and C_4 for β-subtype show negative electrostatic influence for relative binding affinity.

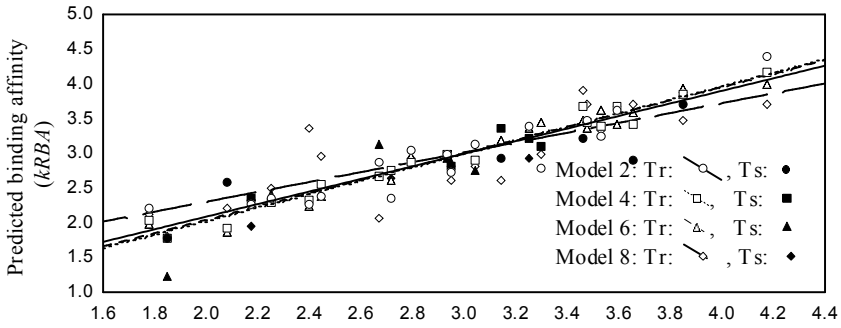

Model 2: Tr: n=17, R^2=0.906, se=0.241, Q^2=0.876
Ts: n=6, R^2_{pred}=0.764, s_p=0.478
Model 4: Tr: n=17, R^2=0.970, se=0.142, Q^2=0.544
Ts: n=6, R^2_{pred}=0.642, s_p=0.359
Model 6: Tr: n=17, R^2=0.956, se=0.160, Q^2=0.663
Ts: n=6, R^2_{pred}=0.693, s_p=0.326
Model 8: Tr: n=17, R^2=0.867, se=1.364, Q^2=0.831
Ts: n=6, R^2_{pred}=0.687, s_p=0.534

Figure 3
Observed vs predicted binding affinity as per QSAR and pharmacophore models for ER β-subtype.

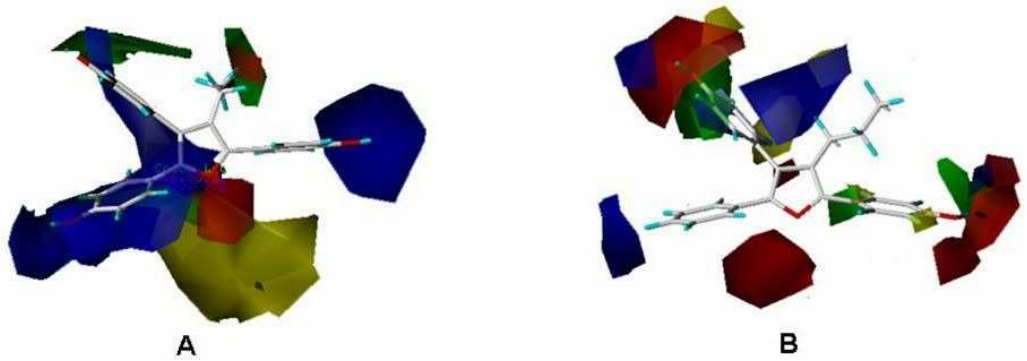

(A) Steric: Green favorable, yellow unfavorable
Electrostatic: Blue favorable, red unfavorable
(B) Steric: Green favorable, yellow unfavorable
Electrostatic: Blue favorable, red unfavorable

Figure 4
CoMFA studies of α- (A, Model 3) and β- (B, Model 4) subtype.

CoMSIA

Best models are developed with 's', 'p' and 'a' factors for both α- (**Model 5**, R^2=0.995, se=0.096, Q^2=0.691, R^2_{bs}=0.999, s_b=0.041, R^2_{pred}=0.580, s_p=0.461) and β-(**Model 6**, R^2=0.956, se=0.160, Q^2=0.663, R^2_{bs}=0.972, s_b=0.118, R^2_{pred}=0.693, s_p=0.326) subtypes. Additionally, 'd' and 'e' are important in Models 5 and 6 respectively. The contribution of 's', 'p', 'a' and 'd' are found as 21.50, 29.70, 24.20 and 24.60% respectively in Model 5, whereas 6.70, 33.30, 10.80, and 49.20% are obtained for 's',

'e', 'p' and 'a' respectively in Model 6. The selected models are used to predict activity of test compounds and found good correlation (R^2_{pred}=0.580 and 0.693 in Models 5 and 6 respectively) between observed and predicted activities, which confirms robustness of the models.

(A)	Steric:	Green favorable, yellow unfavorable
	Hydrophobic:	Blue favorable, red unfavorable
	Acceptor:	Magenta favorable, White unfavorable
	Donor:	Cyan favorable, purple unfavorable
(B)	Steric:	Green favorable, yellow unfavorable
	Electrostatic:	Cyan favorable, purple unfavorable
	Hydrophobic:	Blue favorable, red unfavorable
	Acceptor:	Magenta favorable, White unfavorable

Figure 5
CoMSIA studies of α- (A, Model 5) and β- (B, Model 6) subtype.

Contour maps (Figure 5) suggest that aromatic ring 'B' in both Models 5 and 6, 'C' in Model 5, 'A' in Model 6 along with region around C_6 in Model 6 show positive influence for steric interactions. But regions around O_1 in Model 5, and aromatic rings 'A' and 'C' along with alkyl group at C_3 are unfavourable for steric influence at active site cavity. All three phenyl rings, 'A', 'B' and 'C' are favourable for hydrophobic interactions with amino residues at active site of both subtypes receptor, but rest surface area show negative impact for the interactions. Oxo functional groups at C_{21} in both Models 5 and 6, and C_9 in Model 6 behave as HB acceptors, suggesting the presence of electron rich groups form hydrogen bond interactions. Vicinity to atom C_{21} revealed as important for HB donor in Model 5, while region surrounding the phenyl ring 'C' indicates as unfavorable for HB donor. Phenyl rings 'A' and 'C' along with alkyl group at C_3 position show electrostatically favourable, but surface around O_1 reveals as unfavourable for electrostatic interactions. Observed and predicted activities are delineated in Figures 2 and 3 for α- and β-subtypes respectively.

PHARMACOPHORE STUDY

The best models (**Model 7**, R^2=0.941, *se*=1.250, Q^2=0.872, R^2_{pred}=0.721, s_p=0.443 and **Model 8**, R^2=0.867; *se*=1.364, Q^2=0.871, R^2_{pred}=0.687, s_p=0.534 for α- and β-subtypes respectively) are described in Figure 6. It is revealed that hydrogen bond (HB) donor (d) and hydrophobic (p) features are important in both Models 7 and 8. Additionally HB acceptor (a) in Model 7 and aromatic ring ('r') feature in Model 8 are crucial for selective binding affinity. The configuration cost of the Models 7 and 9 are found to be 14.871 and 13.909; whereas Δ_{cost} (Null cost – Total cost) are observed as 235.052 and 87.601 for α- and β-subtypes respectively. Both the models are validated through Fischer's

randomization test[37] at 95% confidence level. But no other models develop better hypothesis in comparison to original Models 7 and 8.

The bulky R_3-substituent (Figure 1) in both Models 7 and 8, and phenyl rings 'B' and 'C' in Model 7 are found as important for imparting the hydrophobic property of the molecules. The hydroxyl group attached to ring 'B' reduces electron density around it and behaves as HB donor for both α- and β-subtypes. The oxo functional group at position 1 in Model 7 is revealed as crucial for HB interaction at the active site of the receptor. The aromatic rings 'B' and 'D' have positive impact on binding affinity for β-subtype. The inter-feature distances (Figure 6) are also important for interaction at the selective receptor cavity. Correlation (R^2_{pred}) between observed and predicted activity of test set compounds confirms the robustness of the models. Predicted activity of training and test set compounds is depicted in Figures 2 and 3 for Models 7 and 8 respectively.

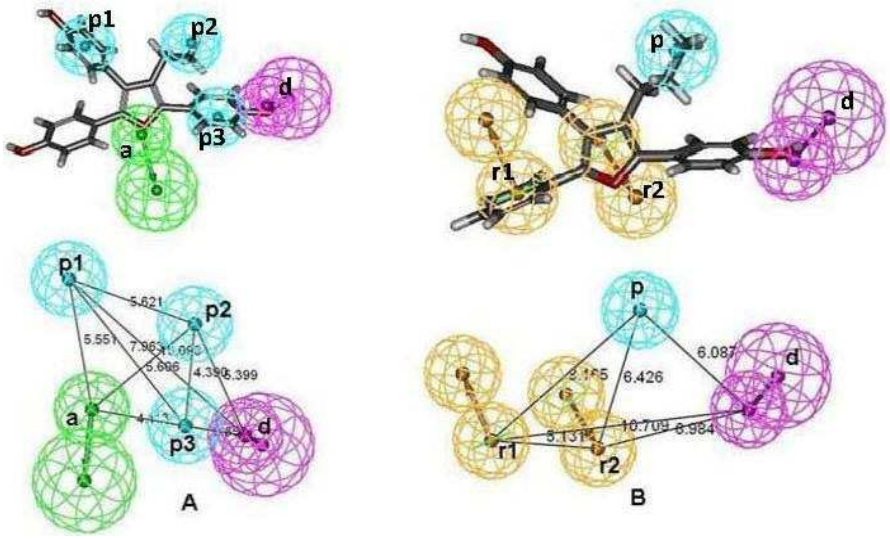

Figure 6

Pharmacophore mapping with most active compound (comp. 7) in training set of α- (A, Model 7) and β- (B, Model 8) subtype. Mapped features: a: HB acceptor, d: HB donor, p: hydrophobic, r: aromatic ring

BINDING INTERACTION

Molecular docking study is performed to correlate chemical functionalities derived from ligand-based modeling for binding interactions at the active site of the receptor. Most active compounds (Comp. **7** in Table 1 for both α- and β-subtypes) are considered as ligands and the crystal structure of receptors (PDB ID: 2R6W[30] and 1L2J[31] for α- and β-subtypes respectively) are used for docking study. The catalytic residues involved for interactions at active site cavity of the α-subtype receptor are Thr347 (polar residue), and Leu346, Leu525 and Leu536 (non-polar residues), whereas Thr299, Glu305 and His475 (polar residues) and, Ile376, Leu380 and Val387 (non-polar residues) are for β-subtype. Binding interactions between ligand and receptor are shown in Figure 7.

In case of α-subtype, importance of steric factor at C_9 in Model 3, and ring 'A' that imparts hydrophobicity in Model 5 are substantiate by HB interactions between hydroxyl group at C_9 with non-polar catalytic residue Leu346 (Figure 7A). Importance of electronic charges at C_8 in Model 1 is adjudged through the bump interaction between C_7 and non-polar Leu346 residue at the active site cavity. It is observed that ring 'C' is important for electrostatic

interaction in Model 3, and steric and hydrophobic properties in Model 5 which validated by HB interaction at C_{21} with non-polar amino residue Leu536. Importance of ring 'B' for steric interaction in Models 3 and 5 are substantiated by forming bump interaction between ring 'B' and polar Thr347 residue. In space modeling study, it is observed that rings 'A' and 'C' along with R_3 substituent impart hydrophobic properties that adjudged by bonding interactions at C_9, C_7, C_{21} and C_{24} with Leu346, Leu525, Leu536 and Thr347 respectively.

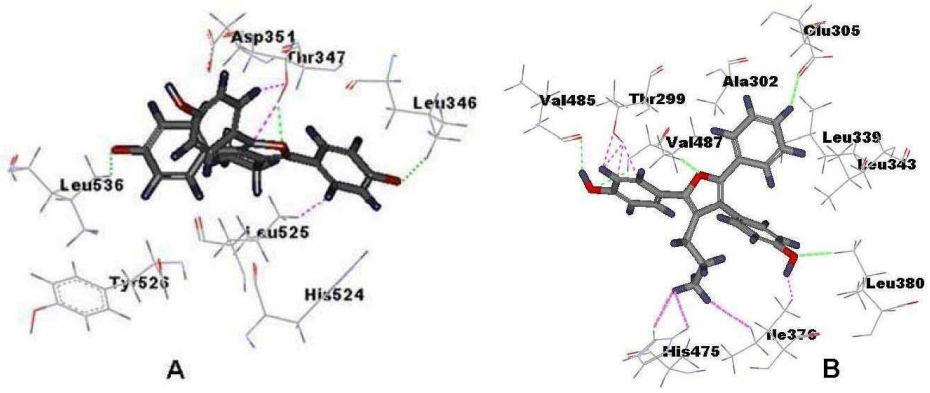

Figure 7
Molecular docking interactions at the binding site of α- (A, PDB ID: 2R6W[30]) and β-subtypes (B, PDB ID: 1L2J[31]).

In case of β-subtype, importance of electronic charges for binding affinity in Model 2, hydroxyl group at C_{21} for steric interaction in Model 4, HB acceptor in Model 6, and hydrophobic property of ring 'C' in Model 6 are confirmed by forming potential bonding at C_{21} with catalytic residue Leu380 (Figure 7B). Electrostatically favorable C_9 position in Model 4 is successfully validated by bonding interactions at C_8 with polar catalytic residue Thr299. Importance of electronic charge of C_{24} in Model 2 is adjudged by forming potential bump interactions at C_{24} position with Ile376 and His475 amino acid residues. Pharmacophore study revealed that R_3 substituent and ring 'D' are important for hydrophobic factors which substantiated by potential interactions at substituent at C_{24} and O_1 with Val485 and Val487 respectively. Hydroxyl group at C_9 behaved as HB donor that is adjudged by HB interaction between hydroxyl group at C_9 with non-polar Val485.

CONCLUSION

In the study, QSAR models involving 2D QSAR, CoMFA and CoMSIA approaches with pharmacophore space modeling for non-steroidal furan and pyrazole analogs are being evaluated that highlighted some of the molecular properties and structural requirement for selective binding affinity to the ER subtypes. QSAR models are generated to find chemical functionalities that expedite molecular features with biological activity. Pharmacophore maps are also generated to search pharmacophoric elements responsible for specific binding affinity to ER-subtypes. It is revealed that electronic charges of C_2, C_4, C_8, C_{18} and C_{24} are crucial for binding affinity. Moreover ring systems in the dataset are imparting hydrophobicity of the molecules. Hydroxyl group present in the molecule is prime factor for forming potential interaction at the active site cavity of the selective ER.

ACKNOWLEDGEMENT

One of the authors, Md A. Islam wishes to thank CSIR, New Delhi, India for awarding Senior Research Fellowship.

REFERENCES

1. Lewis JS and Jordan VC, Selective estrogen receptor modulators (SERMs): mechanisms of anticarcinogenesis and drug resistance. Mutat Res, 591 (1-2): 247-263, (2005).
2. Rossouw JE, Anderson GL, Prentice RL, LaCroix AZ, Kooperberg C, Stefanick ML, Jackson RD, Beresford SA, Howard BV, Johnson KC, Kotchen JM and Ockene J, Risks and benefits of estrogen plus progestin in healthy postmenopausal women: principal results From the Women's Health Initiative randomized controlled trial. JAMA, 288 (3): 321-333, (2002).
3. Gehrig PA, Bae-Jump VL, Boggess JF, Groben PA, Fowler WC Jr. and Van Le L, Association between uterine serous carcinoma and breast cancer. Gynecol Oncol, 94 (1): 208-211, (2004).
4. Chlebowski RT, Hendrix SL, Langer RD, Stefanick ML, Gass M, Lane D, Rodabough RJ, Gilligan MA, Cyr MG, Thomson CA, Khandekar J, Petrovitch H and McTiernan A, Influence of estrogen plus progestin on breast cancer and mammography in healthy postmenopausal women: the Women's Health Initiative Randomized Trial. JAMA, 289 (24): 3243-3253, (2003).
5. Clarke R, Liu MC, Bouker KB, Gu Z, Lee RY, Zhu Y, Skaar TC, Gomez B, O'Brien K, Wang Y and Hilakivi-Clarke LA, Antiestrogen resistance in breast cancer and the role of estrogen receptor signaling. Oncogene, 22 (47): 7316-7339, (2003).
6. Evans RM, The steroid and thyroid hormone receptor superfamily. Science, 240 (4854): 889-895, (1988).
7. Gustafsson JA, Estrogen receptor beta--a new dimension in estrogen mechanism of action. J Endocrinol, 163 (3): 379-383, (1999).
8. Goldstein SR, Siddhanti S, Ciaccia AV and Plouffe L Jr., A pharmacological review of selective oestrogen receptor modulators. Hum Reprod Update, 6 (3): 212-224, (2000).
9. Burger HG, Selective oestrogen receptor modulators. Horm Res, 53 Suppl 3, 25-29, (2000).
10. Prathipati P and Saxena AK, Characterization of beta3-adrenergic receptor: determination of pharmacophore and 3D QSAR model for beta3 adrenergic receptor agonism. J Comput Aided Mol Des, 19 (2): 93-110, (2005).
11. Dowers TS, Qin ZH, Thatcher GR and Bolton JL, Bioactivation of Selective Estrogen Receptor Modulators (SERMs). Chem Res Toxicol, 19 (9): 1125-1137, (2006).
12. Kapetanovic IM, Computer-aided drug discovery and development (CADDD): in silico-chemico-biological approach. Chem Biol Interact, 171 (2): 165-176, (2008).
13. Smith HM, Knox AJ, Zisterer DM, Lloyd DG and Meegan MJ, Flexible estrogen receptor modulators: synthesis, biochemistry and molecular modeling studies for 3-benzyl-4,6-diarylhex-3-ene and 3,4,6-triarylhex-3-ene derivatives. Med Chem, 3 (2): 135-155, (2007).
14. Lewis DF, Parker MG and King RJ, Molecular modelling of the human estrogen receptor and ligand interactions based on site-directed mutagenesis and amino acid sequence homology. J Steroid Biochem Mol Biol, 52 (1): 55-65, (1995).
15. Mukherjee S, Saha A and Roy K, QSAR of estrogen receptor modulators: exploring

selectivity requirements for ER(alpha) versus ER(beta) binding of tetrahydroisoquinoline derivatives using E-state and physicochemical parameters. Bioorg Med Chem Lett, 15 (4): 957-961, (2005).
16. Mukherjee S, Nagar S, Mullick S, Mukherjee A and Saha A, Pharmacophore mapping of selective binding affinity of estrogen modulators through classical and space modeling approaches: exploration of bridged-cyclic compounds with diarylethylene linkage. J Chem Inf Model, 47 (2): 475-487, (2007).
17. Verma J, Khedkar VM and Coutinho EC, 3D-QSAR in drug design--a review. Curr Top Med Chem, 10 (1), 95-115, (2010).
18. Mortensen DS, Rodriguez AL, Sun J, Katzenellenbogen BS and Katzenellenbogen JA, Furans with basic side chains: synthesis and biological evaluation of a novel series of antagonists with selectivity for the estrogen receptor alpha. Bioorg Med Chem Lett, 11 (18), 2521-2524, (2001).
19. Stauffer SR, Coletta CJ, Tedesco R, Nishiguchi G, Carlson K, Sun J, Katzenellenbogen BS and Katzenellenbogen JA, Pyrazole ligands: structure-affinity/activity relationships and estrogen receptor-alpha-selective agonists. J Med Chem, 43 (26): 4934-4947, (2000).
20. Wold S and Eriksson L, *Chemometric Methods*. Vol 2, VCH Verlagsgesellschaft mbh: Weinheim: 312, (1995).
21. Statistica7.1 *StatSoft Inc.*, Tulsa: 2005, http//:www.statsoft.com
22. Cramer III RD, Patterson DE and Bunce JD, Comparative molecular field analysis (CoMFA). 1. Effect of shape on binding of steroids to carrier proteins. J. Am. Chem. Soc., 110: 5959-5967, (1988).
23. Klebe G, Abraham U and Mietzner T, Molecular similarity indices in a comparative analysis (CoMSIA) of drug molecules to correlate and predict their biological activity. J Med Chem, 37 (24): 4130-4146, (1994).
24. Martin Y, 3D QSAR: Current state, scope, and limitations. Perspect Drug Discov Des, 12: 3-23, (1998).
25. Debnath AK, Quantitative structure-activity relationship (QSAR) paradigm--Hansch era to new millennium. Mini Rev Med Chem, 1 (2): 187-195, (2001).
26. Bohm M, St rzebecher J and Klebe G, Three-dimensional quantitative structure-activity relationship analyses using comparative molecular field analysis and comparative molecular similarity indices analysis to elucidate selectivity differences of inhibitors binding to trypsin, thrombin, and factor Xa. J Med Chem, 42 (3): 458-477, (1999).
27. Yang GF and Huang X, Development of quantitative structure-activity relationships and its application in rational drug design. Curr Pharm Des, 12 (35): 4601-4611, (2006).
28. Lushington GH, Guo JX and Wang JL, Whither combine? New opportunities for receptor-based QSAR. Curr Med Chem, 14 (17): 1863-1877, (2007).
29. Dean PM, Lloyd DG and Todorov NP, De novo drug design: integration of structure-based and ligand-based methods. Curr Opin Drug Discov Devel, 7 (3): 347-353, (2004).
30. Dai SY, Chalmers MJ, Bruning J, Bramlett KS, Osborne HE, Montrose-Rafizadeh C, Barr RJ, Wang Y, Wang M, Burris TP, Dodge JA and Griffin PR, Prediction of the tissue-specificity of selective estrogen receptor modulators by using a single biochemical method. Proc Natl Acad Sci U S A, 105 (20): 7171-7176, (2008).
31. Shiau AK, Barstad D, Radek JT, Meyers MJ, Nettles KW, Katzenellenbogen BS, Katzenellenbogen JA, Agard DA and Greene GL, Structural characterization of a subtype-selective ligand reveals a novel mode of estrogen receptor antagonism. Nat Struct Biol, 9 (5): 359-364, (2002).
32. RCSB Proten Data Bank, http://www.rcsb.org/pdb/

33. Kristam R, Gillet VJ, Lewis RA and Thorner D, Comparison of conformational analysis techniques to generate pharmacophore hypotheses using catalyst. J Chem Inf Model, 45 (2): 461-476, (2005).
34. Islam MA, Nagar S, Das S, Mukherjee M and Saha A, Molecular Design Based on Receptor-Independent Pharmacophore: Application to Estrogen Receptor Ligands. Biol Pharm Bull, 31 (1): 1453-1460, (2008).
35. Accelrys Discovery Studio 1.7; 2005, http:// http://accelrys.com/
36. Taha MO, Habash M, Al-Hadidi Z, Al-Bakri A, Younis K, Sisan S, Docking-based comparative intermolecular contacts analysis as new 3-D QSAR concept for validating docking studies and in silico screening: NMT and GP inhibitors as case studies. J Chem Inf Model, 51 (3): 647-669, (2011).
37. Snedecor G, Cochran W, Statistical Methods. Vol 276, Iowa: Iowa State University Press: (1967).